Modelling and Control Design for a High Power Resonant DC-DC Converter

Christoph Hahn[#1], *Member, IEEE,* and Peter Lehn[*2], *Senior Member, IEEE*

[#]*Chair of Electrical Energy Systems, University of Erlangen – Nuremberg, Erlangen, Germany*
[1]christoph.hahn@ees.uni-erlangen.de

[*]*Department of Electrical and Computer Engineering, University of Toronto Toronto, Canada*
[2]lehn@ecf.utoronto.ca

Abstract— **This paper involves the development of a dynamic model for a resonant dc-dc converter topology recently proposed at the University of Toronto. The model makes use of the conservation of energy principle.**
This dynamic model employs an averaging technique, since converter switching is neglected. A simple test network for validation of the proposed model is developed. Based on the validated model, a concept for closed loop control of the system, including the selection of which variables are optimal to control, is determined.

***Keywords*— modelling, control design, dc-dc converters, step-up ratios, average model and switching frequency.**

I. INTRODUCTION

Recently, the desire to use dc bus interconnections has gained interest. The reason for this interest is the increased need to connect dc power sources in the kilowatt and megawatt power range. For example, integrating offshore wind farms through dc networks or providing additional access points to existing HVDC (High-Voltage Direct current) lines. The advantage of using a high power dc-dc converter instead of a VSC (Voltage Source Converter) or a LCC (Line Commutated Converter) is that there is no additional intermediate ac conversion stage required. These converter topologies directly interconnect dc buses of different voltage levels.

Renewable energy production has been progressively increasing as of late as international goals to reduce environmental pollution through carbon dioxide emissions or other greenhouse gases come into effect [1]. To transmit power from certain types of renewable energy generators, such as offshore wind farms, it is necessary to transform the electrical energy to high voltage dc. Currently this is done by using dc-ac converters at the wind turbine, ac transformers followed by ac-dc conversion [2]. The objective of high power dc-dc conversion is to replace these multiple conversion stages with a single, lower cost converter, which is even higher efficient.

In 2010 a new type of resonant dc-dc converter was proposed by University of Toronto [3]. This type of converter was based on another topology proposed at the University of Aberdeen [4].

This paper addresses the problem of finding a mathematical model suitable for control design. With the proposed model, systematic controller design can be carried out. The results of modeling and control design will be shown and discussed for the application. This application is for the interconnection of a power source, like an offshore wind farm, with a high power dc distribution grid. Integration of renewable sources with high power resonant dc-dc converters was discussed in [5].

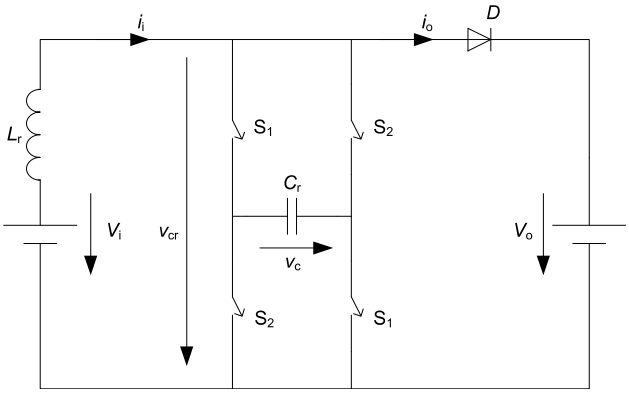

Figure 1: Simplified structure of the step-up converter

Figure 1 shows the recently by University of Toronto proposed step-up converter [3].

The converter is a frequency controlled circuit. It can step up the input voltage v_i to the level of the output voltage v_o without changing the polarity; hence its function is similar to the classical boost converter. However, it is not possible to use similar modeling techniques to the boost converter due to the fact that the converter operates in a resonant mode with frequency control. The converter only operates in the DCM mode so it won't experience forced current chopping during commutation. It contains a resonant inductor, L_r, which is connected to the input bus. In addition, it also has an integrated resonant capacitive active switching network, C_r, and an output diode valve.

978-1-4673-2673-5/12/$31.00©2012IEEE

II. Converter Modelling

Averaging and small-signal linearization are the key steps in modelling converters [6]. Several modelling techniques are presented for resonant converters [7], [8]. The fundamental rules which every converter must obey place constraints on the development of a simpler converter model. Energy and power balance are included in these fundamental rules. Input and output energy, and power, have to be equal if it is assumed that the converter is lossless. This implies converter switching losses should be neglected, no snubbers are assumed and all the converter elements are ideal. Hence it is possible to determine the equations of energy balance for the recently proposed converter [3]:

$$
\begin{aligned}
W_i^* &= W_o^* \\
V_i \int_0^{\gamma/\omega_r} i_C dt + V_i \int_{\gamma/\omega_r}^{T_S/2} i_o dt &= V_o \int_{\gamma/\omega_r}^{T_S/2} i_o dt \\
V_i \int_{-V_o}^{V_o} C_r dv_C + V_i \int_{\gamma/\omega_r}^{T_S/2} i_o dt &= V_o \int_{\gamma/\omega_r}^{T_S/2} i_o dt \\
\rightarrow \int_{\gamma/\omega_r}^{T_S/2} i_o dt &= \frac{2V_i V_o C_r}{V_o - V_i} \\
\rightarrow W_i^* = W_o^* &= \frac{2V_i V_o^2 C_r}{V_o - V_i} \\
\rightarrow W_i = W_o &= \frac{4V_i V_o^2 C_r}{V_o - V_i}
\end{aligned}
\tag{1}
$$

Where W_i^* and W_o^* are the input and output energy per half cycle; W_i and W_o are the input and output energy per full cycle. By multiplying the energy equation by the switching frequency f_s one yields the power equation of the converter.

$$
P_i = P_o = \frac{4V_i V_o^2 C_r f_s}{V_o - V_i} \tag{2}
$$

Dividing the output power $P_o = V_o I_o$ by the output voltage V_o provides an equation which presents some kind of average output current.

$$
I_o = \frac{4V_i V_o C_r f_s}{V_o - V_i} \tag{3}
$$

Using energy or power balance yields the first equation of the converter model. For obtaining another equation describing the circuit one has to look to another fundamental property the converter is based upon. For this converter, since it only operates in DCM, the general shape of the current waveforms can be utilized to come up with the second equation for the converter model.

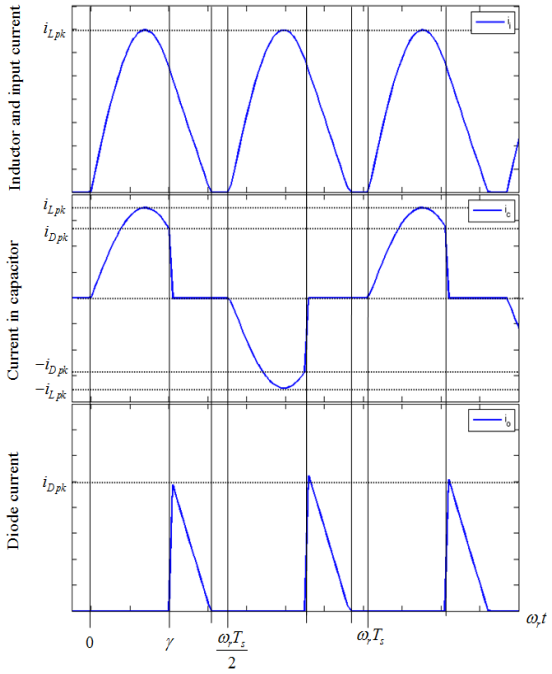

Figure 2: Ideal steady state waveforms for the step-up converter

Looking at the waveforms in Figure 2 and using Equation (3) one obtains the equation for the average input current.

$$
\begin{aligned}
I_i &= \frac{2}{T_S} \int_0^{\gamma/\omega_r} i_C dt + \underbrace{\frac{2}{T_S} \int_{\gamma/\omega_r}^{T_S/2} i_o dt}_{I_o} = \frac{2}{T_S} C_r \int_{-V_o}^{V_o} dv_C + I_o \\
I_i &= 4 f_s C_r V_o + I_o
\end{aligned}
\tag{4}
$$

According to these equations the converter equivalent circuit diagram can be presented in the following way.

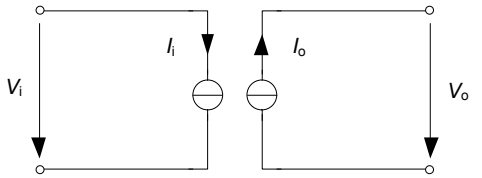

Figure 3: Equivalent circuit diagram for the step-up converter

Its appropriate set of equations can be summarized from the Equations (3) and (4). They describe the entire behaviour of the converter in the DCM mode.

A. Assumptions

For the modeling converters there are assumptions to which they are subject. For the step-up converter model two assumptions are important.

- By using the concept of conservation of energy, over one period at resonant frequency, one neglects the variation in the energy storage within the converter. Multiplying the energy with the switching frequency yields the power balance. By using power balance there is no way to model something like energy storage in the model, but there is energy stored in the capacitor. This is also the reason for the first constraint of using this model. If the output voltage changes too fast, the energy in the capacitor needs to increase. The entire current will flow into the capacitor, increasing the voltage across the capacitor; hence there is no output current for a short period.
- The second fundamental assumption is used when comparing the input and output current shapes. By this process one could detect, that the output current is just a part of the input current; hence the second model equation is found. When choosing this approach one has to be aware that all losses in the converter are neglected.

B. Constraints and Limitations

The use of the concept of the conservation of energy principle, and analysis of the current waveforms to model the converter has its consequences. The reason for these consequences arise since the energy storage in the resonant capacitor and inductor are not included in the model.

- The output voltage is not allowed to change too fast, because in the real converter the voltage across the resonant capacitor is not able to follow as fast as the output voltage might increase; hence the output current will decrease to zero for a brief interval. This is not represented in the mathematical model, since energy storage in the converter is neglected. The output current will converge to the correct steady state value, but the transient current will not drop to zero.
- The output voltage must always be higher than the input voltage, otherwise there is a pole in the calculation and the input current as well as the output current will rise unbounded. This is not only a model limit; it is also a converter limit. The converter cannot operate in an area where both voltages are equal. This physical limit is mapped in a mathematical equation.

$$I_o = \frac{4V_iV_oC_rf_s}{V_o - V_i} \xrightarrow{V_i = V_o} \inf$$
$$I_i = 4f_sC_rV_o + I_o \xrightarrow{V_i = V_o} \inf \quad (5)$$

These two constraints limit the operating range of the converter model. Using it for very fast current and voltage build up processes might neglect some dynamic behavior.

III. CONTROL DESIGN

After developing a mathematical model for the resonant step up converter it follows that one should investigate the suitability of the model for control design. It can only be valid for a certain range of operating conditions. This range was qualitatively discussed in the constraints and limitations section. This section will involve determination of the limits of operation imposed by using the developed mathematical model. Also, the best operating range of the converter is determined. Figure 4 shows the control structure of the system with the integrated converter model.

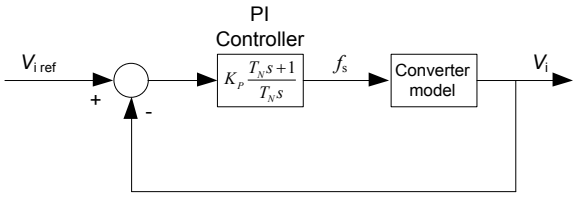

Figure 4: Control structure of the system

To investigate the dynamic behavior of the converter, along with the robustness of the mathematical model, it is important to choose a converter that has a matching input and output circuit.

For a high power application one could imagine connecting several wind turbines or a grid of solar panels to the input of the converter. The output could then be connected to a medium or high voltage dc cable, which would connect the dc-dc converter to a remote VSC. As a simple case study, an off-shore wind farm with a $150\,kV$ submarine cable [9] connection will be investigated. Figure 5 shows a representative model for this case study.

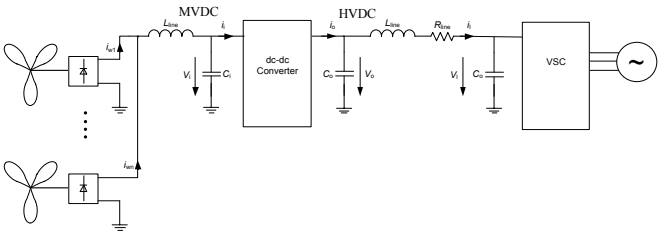

Figure 5: Application of dc-dc Converter in offshore wind farm

Wind farms and solar arrays can each be modeled by an equivalent current source. The current source will have varying amplitudes depending on the present environmental conditions. The purpose of the modeled converter is to step up a voltage in order to transmit the electrical energy over long distances at minimized losses on a high voltage dc bus. For offshore wind farms, the method of transmission would be through a high voltage dc submarine cable, which is typically at least $100\,km$ long. Behind the high voltage transmission line there is typically a high power VSC which converts the dc voltage of the converter to a three phase ac voltage. The VSC controls the dc voltage at its input; hence a simplified model for the VSC is a voltage source. The simplified system is shown in Figure 6.

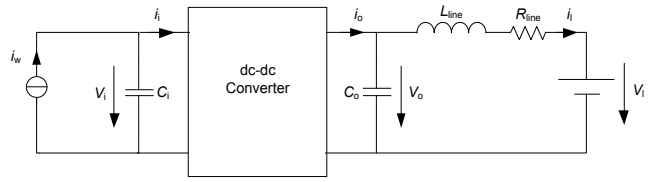

Figure 6: Converter model in order to connect an offshore wind farm to a VSC

The nominal values for the converter elements regarding to its previously mentioned application are $P_n = 60\,\text{MW}$, $i_w = 1818\,\text{A}$, $v_l = 150\,\text{kV}$, $C_r = 3.376\,\text{mF}$, $L_r = 9.298\,\text{mH}$, $C_i = 800\,\text{mF}$, $C_o = 80\,\text{mF}$, $f_s^n = 700\,\text{Hz}$, $V_i^n = 33\,\text{kV}$, $V_o^n = 150\,\text{kV}$, $L_{line} = 68\,\text{mH}$ and $R_{line} = 11.48\Omega$, from [3], [6] and [9].

The dynamics of this new system are described by the differential equations of Figure 6 and the model equations of (3) and (4).

$$\begin{aligned} C_i \frac{dV_i}{dt} &= i_w - i_i = -4V_o C_r f_s - \frac{4C_r f_s V_o V_i}{V_o - V_i} + i_w \\ C_o \frac{dV_o}{dt} &= i_o - i_l = \frac{4C_r f_s V_o V_i}{V_o - V_i} - i_l \\ L_{line} \frac{di_l}{dt} &= V_o - V_l - i_l R_{line} \end{aligned} \tag{6}$$

Equation (6) shows the three states of the system. These differential equations are highly non-linear and need to be linearized. This can be done through use of the Taylor series decomposition method, where the differential terms with orders greater than one are neglected.

$$\begin{aligned} \Delta\dot{\mathbf{x}} &= \begin{pmatrix} \Delta\dot{V}_i \\ \Delta\dot{V}_o \\ \Delta\dot{i}_l \end{pmatrix} = \\ &= \underbrace{\begin{pmatrix} -\frac{4C_r f_s^n (V_o^n)^2}{C_i \left(V_o^n - V_i^n\right)^2} & -\frac{4C_r f_s^n \left((V_o^n)^2 - V_o^n V_i^n\right)}{C_i \left(V_o^n - V_i^n\right)^2} & 0 \\ \frac{4C_r f_s^n (V_o^n)^2}{C_o \left(V_o^n - V_i^n\right)^2} & -\frac{4C_r f_s^n (V_i^n)^2}{C_o \left(V_o^n - V_i^n\right)^2} & \frac{-1}{C_o} \\ 0 & \frac{1}{L_{line}} & \frac{-R_{line}}{L_{line}} \end{pmatrix}}_{\mathbf{A}} \underbrace{\begin{pmatrix} \Delta V_i \\ \Delta V_o \\ \Delta i_l \end{pmatrix}}_{\Delta\mathbf{x}} + \\ &+ \underbrace{\begin{pmatrix} -\frac{4C_r (V_o^n)^2}{C_i \left(V_o^n - V_i^n\right)} & \frac{1}{C_i} & 0 \\ \frac{4C_r V_o^n V_i^n}{C_o \left(V_o^n - V_i^n\right)} & 0 & 0 \\ 0 & 0 & \frac{-1}{L_{line}} \end{pmatrix}}_{\mathbf{B}} \underbrace{\begin{pmatrix} \Delta f_s \\ \Delta i_w \\ \Delta V_l \end{pmatrix}}_{\Delta\mathbf{u}} \end{aligned} \tag{7}$$

The dc-dc converter provides voltage regulation of the MVDC network, since no slack bus exists in the off-shore MVDC network. The HVDC line voltage is controlled by the VSC. The VSC is modeled by a voltage source. Figure 7 shows the Bode diagram of the complete system, represented in equation (7). It is essentially a first order delay except for the peak at approximately $400\,\text{rad/sec}$. This peak is the result of adding the transmission line to the model.

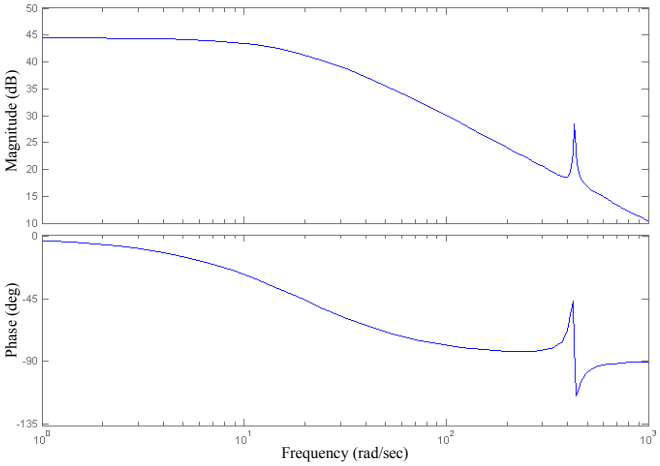

Figure 7: Bode diagram of the complete system

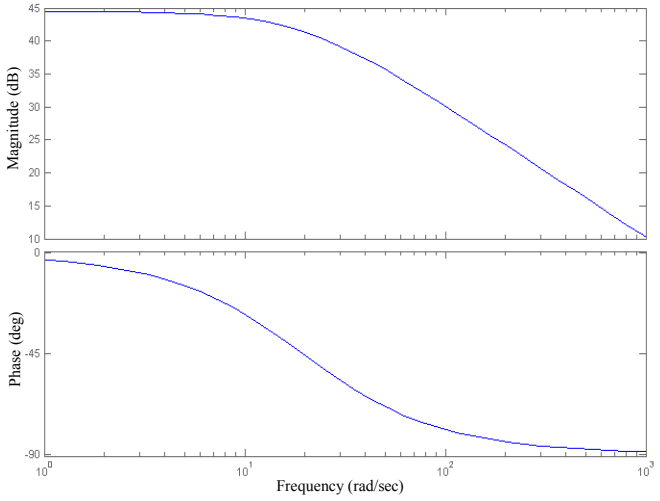

Figure 8: Bode plot of the simplified system

A simple converter controller can be designed by using only the first row of the **A** and **B** matrices. These rows yield a sufficiently accurate transfer function of the system. Figure 8 shows that this assumption is valid; the Bode diagram is essentially the Bode diagram shown in Figure 7, excluding the peak. The controller will be tuned by linearizing about the half rated load operating point with a switching frequency $f_s = 350Hz$. The values necessary for determining the controller will be normalized to their S.I. units.

$$\Delta V_i = \frac{-\frac{b_{11}}{a_{11}}\Delta f_s - \frac{b_{12}}{a_{11}}\Delta i_w}{1-\frac{s}{a_{11}}} = \frac{-334.3\Delta f_s + 128.4\Delta i_w}{1+\frac{s}{9.71}} \quad (8)$$

Equation (8) is represented by a first order delay; as such a controller can be readily designed, e.g. by the method of design with the help of the frequency response characteristic.

IV. Results

The response of the controlled system when the controller parameters of equation (9) are used is shown in Figure 9.

$$F_{PI}(s) = 0.43\frac{0.003\sec s + 1}{0.003\sec s} \quad (9)$$

The voltage v_i of the MVDC network is regulated at $33kV$. The controller has to handle five $300A$ step-up changes in the wind turbine current at $t_1 = 2.0\sec$, $t_2 = 4.0\sec$, $t_3 = 6.0\sec$, $t_4 = 7.0\sec$ and $t_5 = 8.0\sec$; starting at $i_w = 318A$ and ending at $i_w = 1818A$; which is the rated input current of the converter. This scenario could represent the powering-on process of multiple wind turbines in the off-shore wind farm. The converter currents and voltages have to remain stable and within certain bounds during this turning on process in order to guarantee accurate operation.

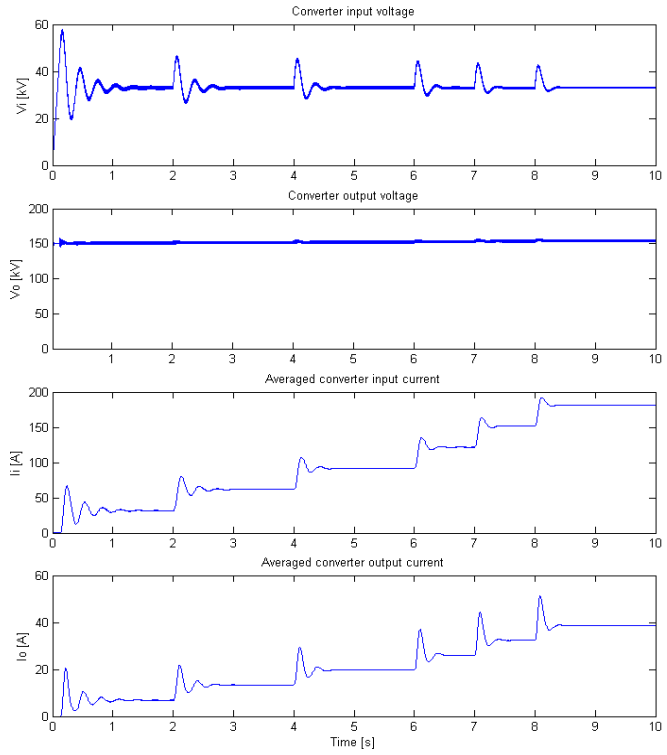

Figure 9: Closed loop responses with optimized controller

Equation (7) shows the system matrix **A** of the entire system. The eigenvalues of **A** can be calculated and plotted with MATLAB® and the results are shown in Figure 10 (blue). Every eigenvalue is plotted eight times for switching frequencies f_s starting by $100Hz$ and ending by $800Hz$.

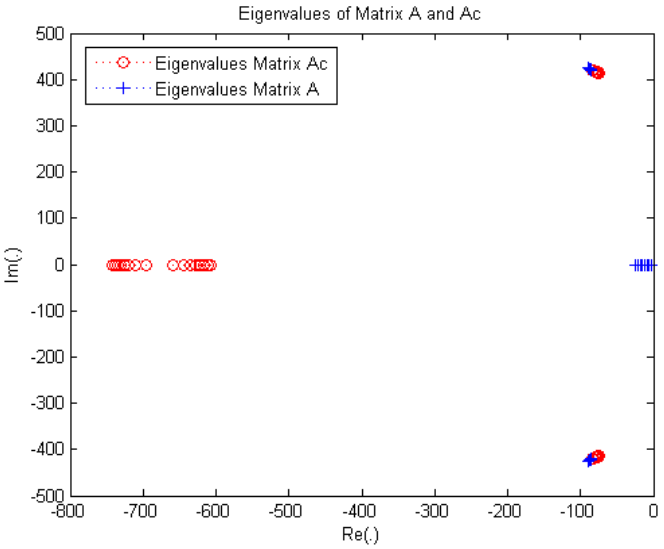

Figure 10: Eigenvalues of the closed and open loop system

The system has three eigenvalues; a pair of complex conjugates (which are affected by the transmission line) and a real one (which is affected by the converter). The eigenvalues are determined in equation (10) and (11).

$$e_1 = -\frac{4C_r(V_o^n)^2}{C_i\left(V_o^n - V_i^n\right)^2} f_s \approx -0.028 f_s \quad (10)$$

$$e_{2,3} = -\frac{R_{line}}{2L_{line}} \pm j\frac{1}{\sqrt{L_{line}C_o}} \approx -84.41 \pm j428.74 \quad (11)$$

The first eigenvalue, e_1, is essentially the first entry a_{11} of the system matrix **A** (this can be observed through an analytic eigenvalue calculation) and hardly depends on the switching frequency at which the converter is operating at. The dynamics of the converter decrease at higher switching frequencies.

To determine the closed loop eigenvalues of the entire system the PI controller along with the converter differential equation has to be included in the calculation.

Inserting the PI controller in the **A** matrix of equation (7) yields a closed loop system description with its system matrix $\mathbf{A_c}$, which is presented in equation (12). The eigenvalues of $\mathbf{A_c}$ are also shown in Figure 10 (red).

$$\mathbf{A_e} = \begin{pmatrix} 0 & K_P & 0 & 0 \\ -\frac{1}{T_N}\frac{4C_r(V_o^n)^2}{C_i\left(V_o^n - V_i^n\right)} & -\frac{4C_r f_s^n (V_o^n)^2}{C_i\left(V_o^n - V_i^n\right)^2} + K_P\frac{4C_r(V_o^n)^2}{C_i\left(V_o^n - V_i^n\right)} & -\frac{4C_r f_s^n\left((V_o^n)^2 - V_o^n V_i^n\right)}{C_i\left(V_o^n - V_i^n\right)^2} & 0 \\ \frac{1}{T_N}\frac{4C_r V_o^n V_i^n}{C_o\left(V_o^n - V_i^n\right)} & \frac{4C_r f_s^n (V_o^n)^2}{C_o\left(V_o^n - V_i^n\right)^2} - K_P\frac{4C_r V_o^n V_i^n}{C_o\left(V_o^n - V_i^n\right)} & -\frac{4C_r f_s^n (V_i^n)^2}{C_o\left(V_o^n - V_i^n\right)^2} & \frac{-1}{C_o} \\ 0 & 0 & \frac{1}{L_{line}} & \frac{-R_{line}}{L_{line}} \end{pmatrix} \quad (12)$$

Figure 10 shows that the controller does not affect the conjugate complex eigenvalues of the system. The input voltage is controlled and therefore does not influence the eigenvalues of the output system. Only the converter eigenvalue e_1 was moved further in the negative real direction implying that the system was sped up by the converter.

V. Conclusions

In this paper, a mathematical model suitable for control design of a new family of dc-dc converters was proposed. It also included the assumptions, constraints, and limitations of the model. Using these, the appropriate operating range of the model was found, as well as the appropriate application for the proposed converter.

Mathematical analysis of the proposed model was carried out. This resulted in a set of design equations allowing accurate determination of the controller parameters. The dynamics of the converter were measured. It was shown that the model equations fit the dynamics of the actual converter. Most of the dynamic behavior exhibited by the converter resemble first order delay behavior and as such the control design is simple.

A simple controller for the converter was determined. It was shown that the dynamics of the input and output voltage and current match those obtained from the mathematical model.

It was observed that the controller does not affect the eigenvalues associated with the transmission line. Any HVDC line dynamics have no major impact on the input circuit of the converter. This implies that the controller does not need to stabilize the dynamics of the output line while controlling the input voltage.

The mathematical model of the step up dc-dc converter was proposed, observed and validated.

References

[1] B. Igielska. *Climate change mitigation: overview of the environmental policy instruments*. International Journal of Green Economics, vol. 2(2): 210-225, 2008.

[2] S. Heier. *Grid Integration of Wind Energy Conversion Systems*. John Wiley & Sons Publishing, West Sussex, England, 2006.

[3] A. Hagar. *A new Family of Transformerless Multi-Module DC-DC Converters for High Power Applications*. PhD thesis, University of Toronto, 2011.

[4] D. Jovcic. *Step-up DCDC converter for megawatt size applications*. IET Power Electron 2009, vol. 2, Iss. 6, pp. 675-685, Nov. 2008

[5] D. Jovcic and B.T. Ooi. *High-Power, Resonant DC/DC Converter for Integration of Renewable Sources*. IEEE Bucharest Power Tech Conference, July 2, 2009.

[6] R. Erickson, D. Maksimovic. *Fundamentals of Power Electronics*. Kluwer Academic Publishers, Boulder, Colorado, 2004.

[7] A. Poleri, Taufik, M. Anwari. *Modeling and Simulation of Paralleled Series-Loades-Resonant Converter*. Second Asia International Conference on Modelling & Simulation, 974-979, 2008.

[8] B. Baha, M.O. Tokhi. *Dynamic Modelling and Control of Resonant Switch Mode Converters*. Control Eng. Practise, vol. 5(11):1533-1542, 1997.

[9] L. Heinhold, R. Stubbe. *Power Cables and their Application*. Published by Siemens Aktiengesellschaft, Berlin and Munich, 1993.

Christoph Hahn received his Dipl.-Ing. degree from the University of Erlangen/Nuremberg, Germany, in 2011. Currently he is a Ph.D. student at the University of Erlangen/Nuremberg, Germany.
In 2010/2011 he did a research project with Prof. Peter Lehn at the University of Toronto.

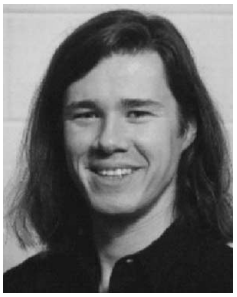

Peter W. Lehn received the B.Sc. and M.Sc. degrees from the University of Manitoba, Winnipeg, MB, Canada, in 1990 and 1992, respectively, and the Ph.D. degree from the University of Toronto, Toronto, ON, Canada, in 1999, all in electrical engineering.
From 1992 to 1994, he was with the Network Planning Group of Siemens AG, Erlangen, Germany. Currently, he is Professor at the University of Toronto.